Electronic Supplementary Information for

Catalytic performance of layered double hydroxide nanosheets toward phenol hydroxylation

Guoqing Cui, Fei Wang, Shan He* and Min Wei*

State Key Laboratory of Chemical Resource Engineering, Beijing University of Chemical Technology, Beijing 100029, P. R. China

* To whom correspondence should be addressed.

Tel.: +8610-64412131; fax: +8610-64425385.

E-mail: vh30@163.com (Shan He); weimin@mail.buct.edu (Min Wei).

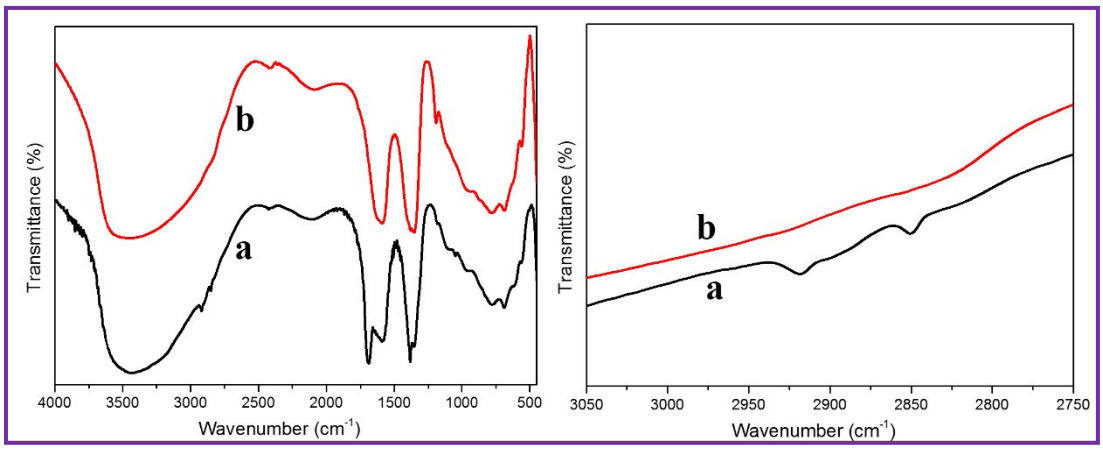

Figure S1. FT-IR spectra of CuMgAl-LDH@mSiO_2 before (a) and after (b) refluxing in acetone.

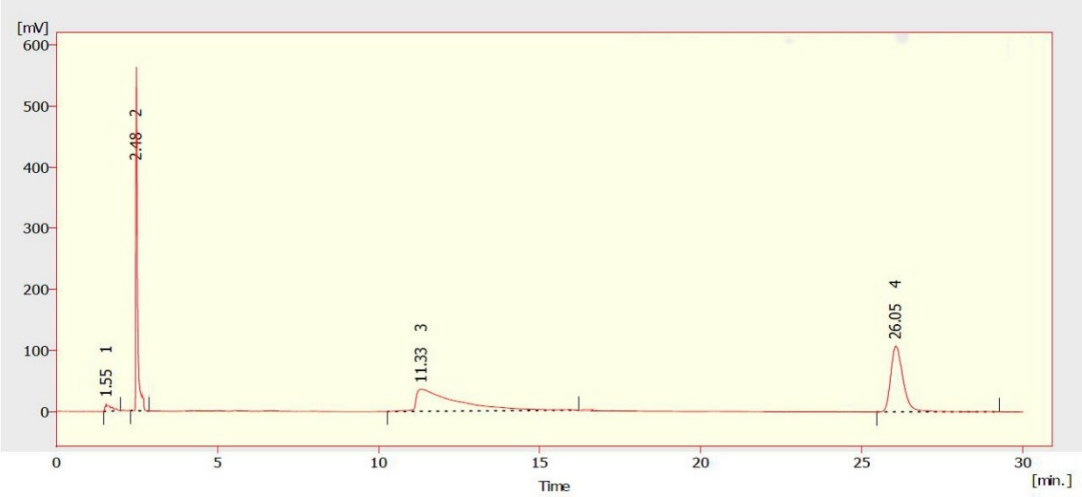

Figure S2. A representative GC profile of the product mixture. From left to right: p-benzoquinone, phenol, catechol and hydroquinone.

The conversion of phenol was calculated by using the following equation:

$$X_{ph} = \frac{n_2 + n_3 + n_4}{n_1 + n_2 + n_3 + n_4} \times 100\% \quad (1)$$

Where n_1, n_2, n_3, n_4 are the molar amount of phenol, catechol, hydroquinone and p-benzoquinone, respectively.

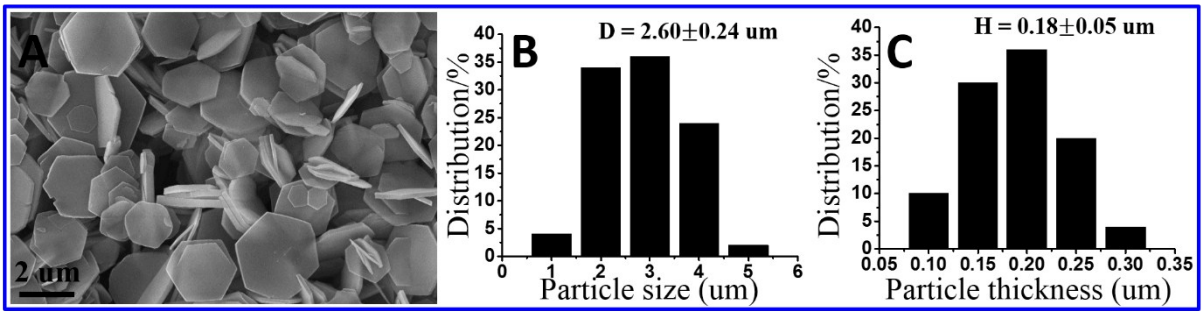

Figure S3. (A) SEM image of U-CuMgAl(CO_3)-LDH; (B) particle size distribution of U-CuMgAl(CO_3)-LDH based on SEM image; (C) particle thickness distribution of U-CuMgAl(CO_3)-LDH based on SEM image.

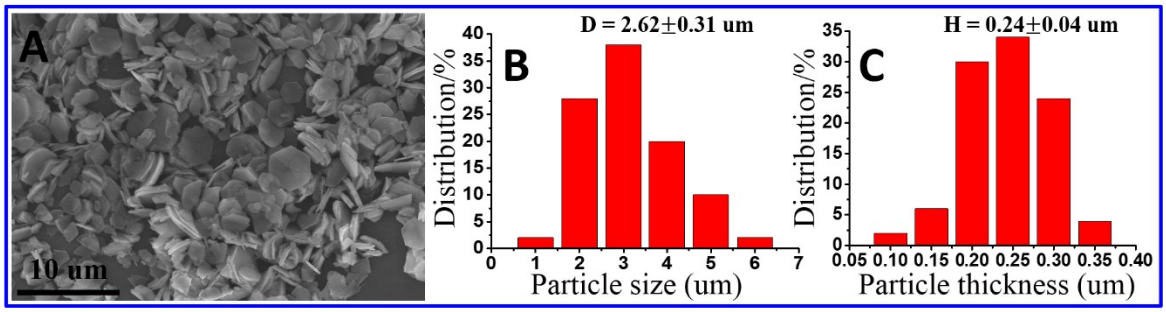

Figure S4. (A) SEM image of U-CuMgAl(NO_3)-LDH; (B) particle size distribution of U-CuMgAl(NO_3)-LDH based on SEM image; (C) particle thickness distribution of U-CuMgAl(NO_3)-LDH based on SEM image.

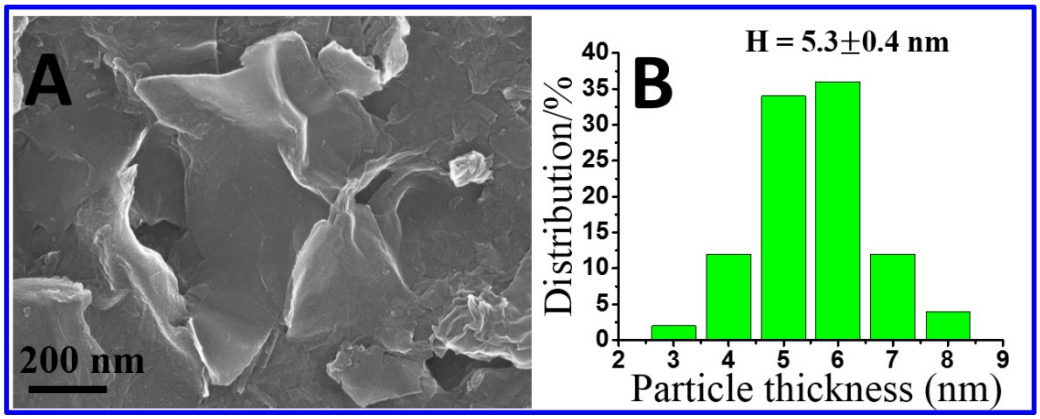

Figure S5. (A) SEM image of CuMgAl-LDH@mSiO_2; (B) particle thickness distribution of CuMgAl-LDH@mSiO_2 based on SEM image.

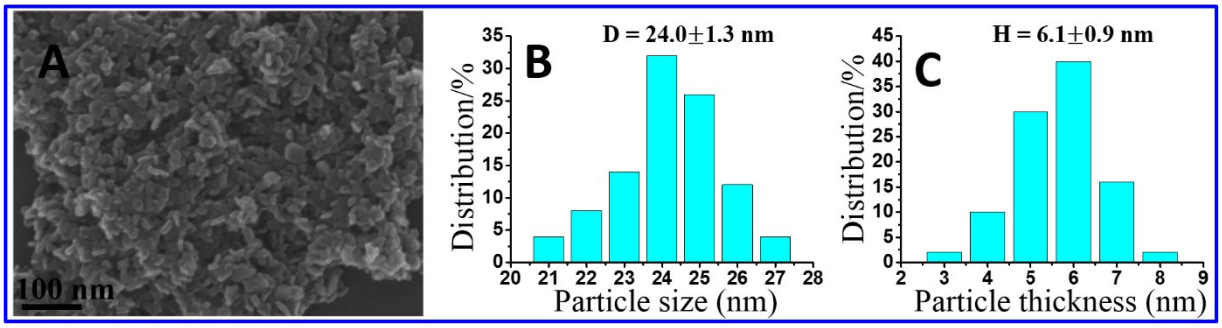

Figure S6. (A) SEM image of S-CuMgAl-LDH-80; (B) particle size distribution of S-CuMgAl-LDH-80 based on SEM image; (C) particle thickness distribution of S-CuMgAl-LDH-80 based on SEM image.

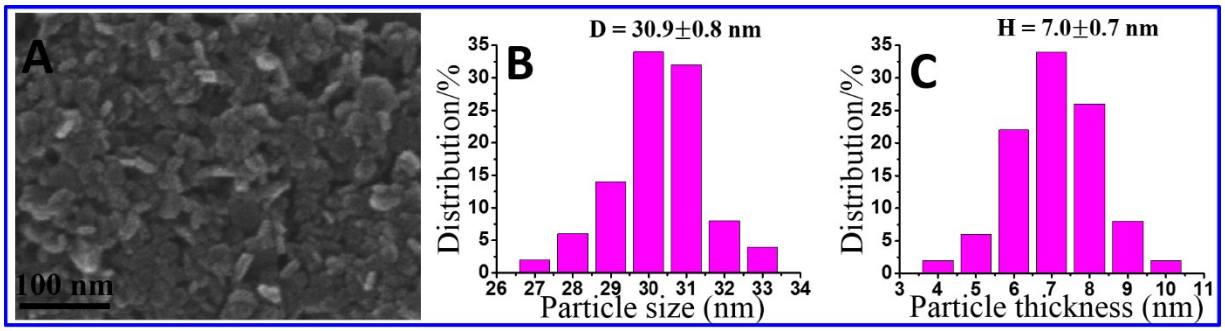

Figure S7. (A) SEM image of S-CuMgAl-LDH-100; (B) particle size distribution of S-CuMgAl-LDH-100 based on SEM image; (C) particle thickness distribution of S-CuMgAl-LDH-100 based on SEM image.

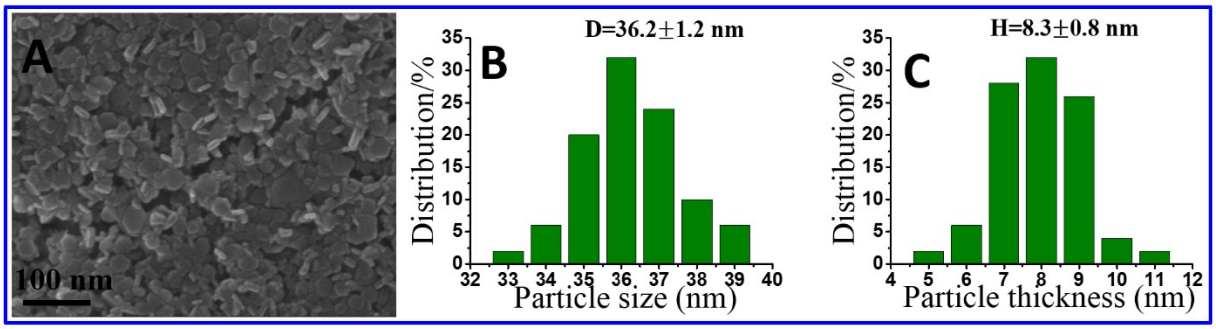

Figure S8. (A) SEM image of S-CuMgAl-LDH-120; (B) particle size distribution of S-CuMgAl-LDH-120 based on SEM image; (C) particle thickness distribution of S-CuMgAl-LDH-120 based on SEM image.

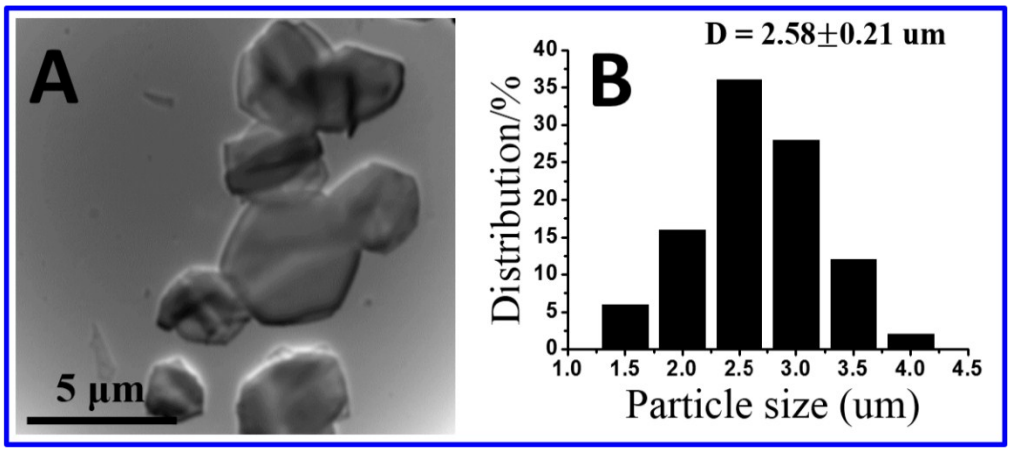

Figure S9. (A) TEM image of U-CuMgAl(CO_3)-LDH; (B) particle size distribution of U-CuMgAl(CO_3)-LDH based on TEM image.

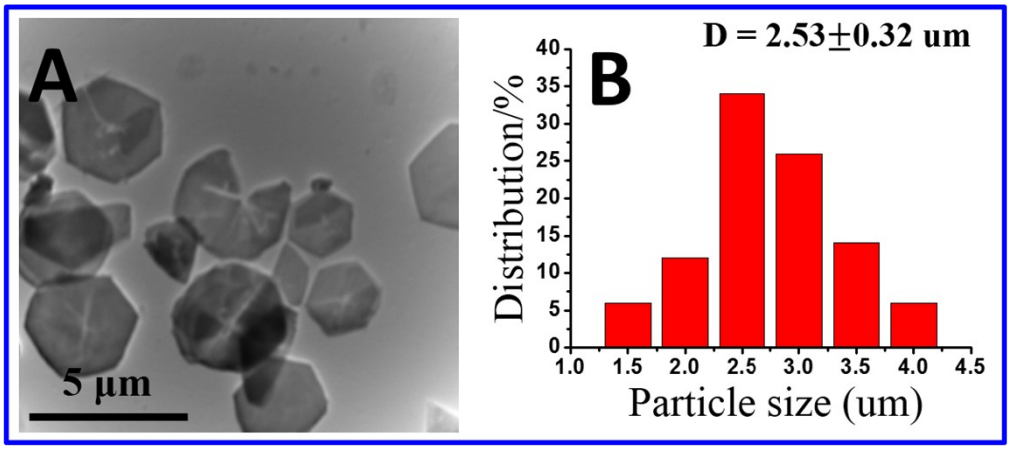

Figure S10. (A) TEM image of U-CuMgAl(NO_3)-LDH; (B) particle size distribution of U-CuMgAl(NO_3)-LDH based on TEM image.

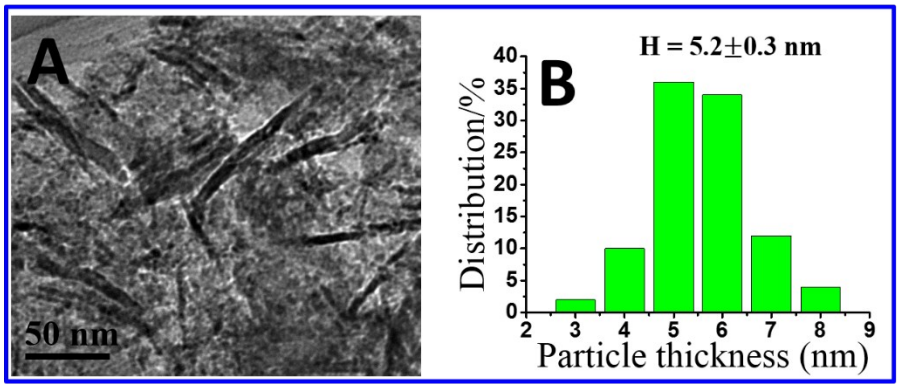

Figure S11. (A) TEM image of CuMgAl-LDH@mSiO_2; (B) particle thickness distribution of CuMgAl-LDH@mSiO_2 based on TEM image.

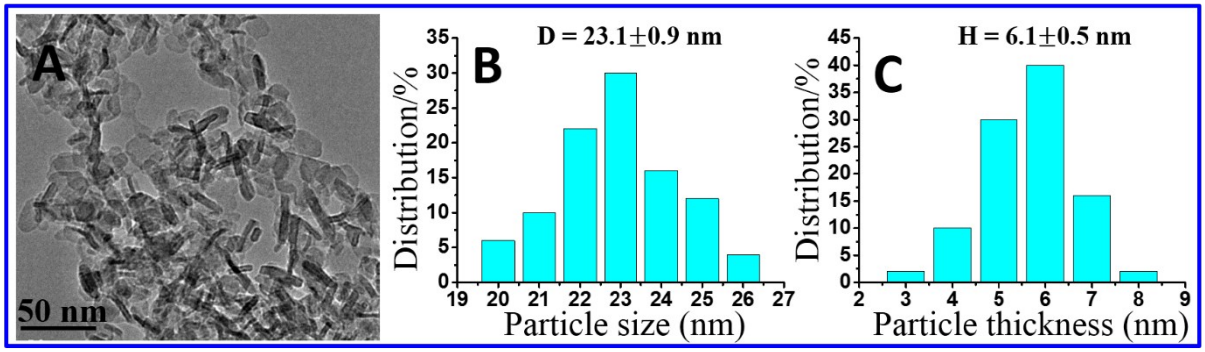

Figure S12. (A) TEM image of S-CuMgAl-LDH-80; (B) particle size distribution of S-CuMgAl-LDH-80 based on TEM image; (C) particle thickness distribution of S-CuMgAl-LDH-80 based on TEM image.

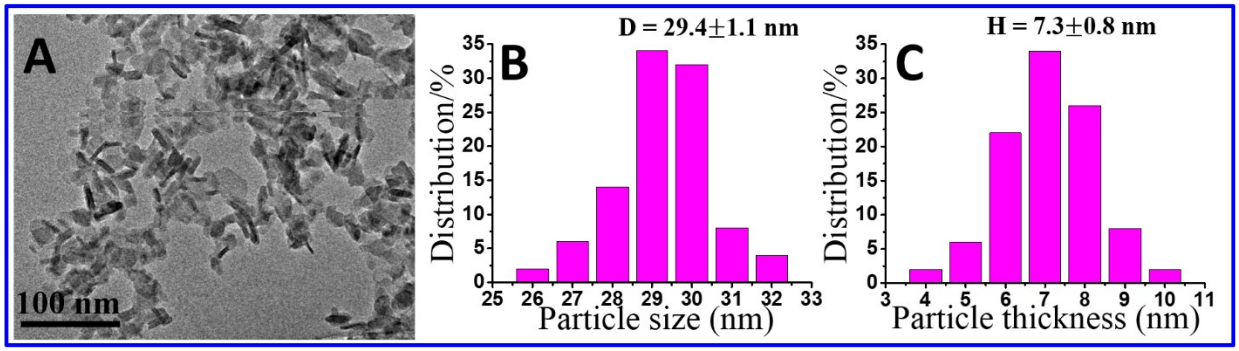

Figure S13. (A) TEM image of S-CuMgAl-LDH-100; (B) particle size distribution of S-CuMgAl-LDH-100 based on TEM image; (C) particle thickness distribution of S-CuMgAl-LDH-100 based on TEM image.

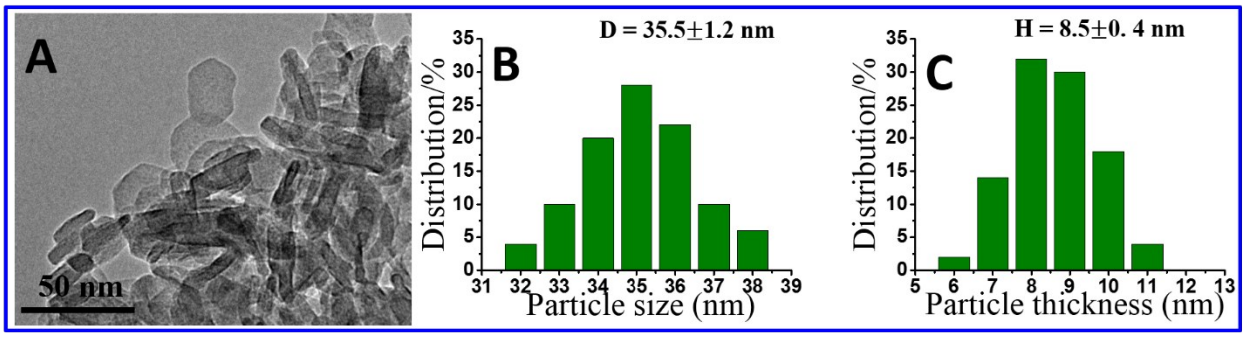

Figure S14. (A) TEM image of S-CuMgAl-LDH-120; (B) particle size distribution of S-CuMgAl-LDH-120 based on TEM image; (C) particle thickness distribution of S-CuMgAl-LDH-120 based on TEM image.

Table S1. N_2 sorption isotherms and pore size distribution of various catalysts

Catalyst	S_{BET} [a] (m^2/g)	D_{BET} [b] (nm)	V_{BET} [c] (cm^3/g)
S-CuMgAl-LDH-80	111.8	9.9	0.280
S-CuMgAl-LDH-100	89.8	10.5	0.240
S-CuMgAl-LDH-120	75.5	15.9	0.260
U-CuMgAl(CO_3)-LDH	17.1	18.8	0.081
U-CuMgAl(NO_3)-LDH	17.3	19.1	0.060
CuMgAl-LDH@$mSiO_2$	244.3	7.6	0.460

[a] S_{BET} represents the specific surface area; [b] D_{BET} represents the average pore size; and [c] V_{BET} denotes the pore volume.

Table S2. Catalytic performance toward phenol hydroxylation over various catalysts

Catalyst	Reaction temperature	molar ratio of phenol/H_2O_2	weight ratio of phenol/ catalyst	Cu content (wt.%)	X_{ph} [a]	S_{CAT+HQ} [b]	H_2O_2 Eff [c] (%)	Normal Activity [d]	Ref.
CuMgAl-LDH@$mSiO_2$	65 °C	1.0	10.0	0.9	58.3	93.4	58.3	423.0	this work
CuMgAl-LDH@$mSiO_2$	65 °C	2.0	10.0	0.9	45.6	97.3	91.1	330.8	this work
CuMgAl-LDH@$mSiO_2$	65 °C	3.0	10.0	0.9	31.2	96.8	93.6	234.1	this work
CuMgAl-LDH@$mSiO_2$	65 °C	5.0	10.0	0.9	19.1	95.7	95.5	143.3	this work
5CuNaY	60 °C	1.0	10.0	2.4	45.3	62.9	45.3	128.0	1
5CuHβ	60 °C	1.0	10.0	1.1	49.3	73.0	49.3	317.1	1
5CuHZSM-5	60 °C	1.0	10.0	1.0	47.0	14.6	47.0	305.2	1
$CuFe_2O_4$−RGO_{20}	55 °C	1.0	94.0	21.2	35.5	95.2	35.5	101.4	2
$CuCl_2$+SiW_{12}	70 °C	0.5	10.0	2.0	38.7	83.9	17.8	130.6	3
[Cu-Imace-H][NO_3]	70 °C	1.0	10.0	--	27.0	99.6	27.0	54.0	4

[a] X_{ph} represents conversion of phenol. [b] S_{CAT+HQ} represents the selectivity toward major products including hydroquinone (HQ) and catechol (CAT). [c] H_2O_2 Eff %=100×(H_2O_2 consumed in the formation of products, mol)/(total H_2O_2 added, mol). [d] Normalized activity value (mol phenol /mol Cu^{2+}) is calculated based on the coverted phenol by per mole of copper.

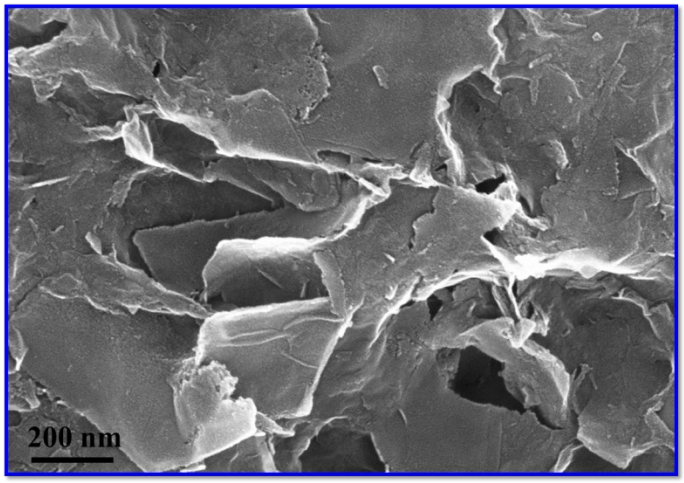

Figure S15. SEM image of the used CuMgAl-LDH@mSiO$_2$ catalyst after four consecutive recycles of phenol hydroxylation.

References:

1 J. Wang, J. N. Park, H. C. Jeong, K. S. Choi, X. Y. Wei, S. I. Hong and C. W. Lee, *Energy & Fuels*, 2004, **18**, 470-476.

2 Y. Zhao, G. He, W. Dai and H. Chen, *Ind. Eng. Chem. Res.*, 2014, **53**, 12566-12574.

3 H. Zhang, X. Zhang, Y. Ding, L. Yan, T. Ren and J. Suo, *New J. Chem.*, 2002, **26**, 376-377.

4 G. Yang, X. Hu, Y. Wu, C. Liu and Z. Zhang, *Catal. Commun.*, 2012, **26**, 132-135.